Ch06 Polymer rheology

- Steady shear flow
  - General effects
  - Material effects
  - Temp and press effects
- Unsteady shear flow
  - Small strain
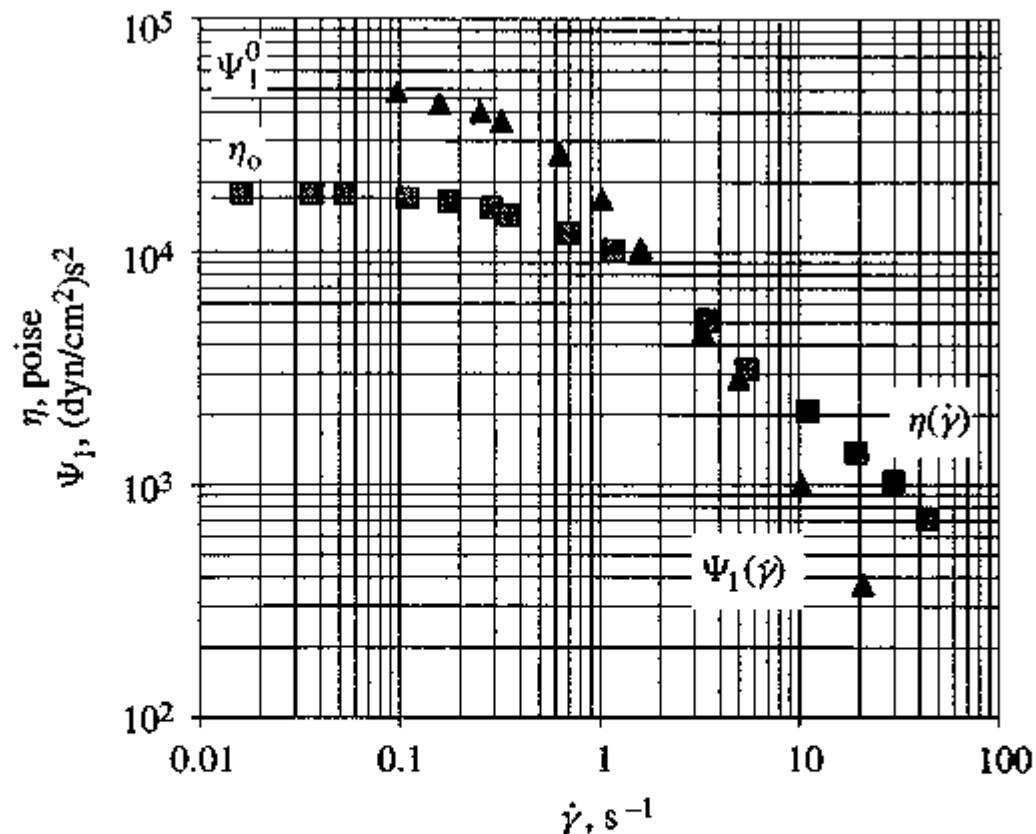 - Large strain
- Elongational flow

Figure 6.1 Steady shear viscosity η and first normal-stress coefficient Ψ_1 as a function of shear rate $\dot{\gamma}$ for a concentrated solution of a narrowly distributed polybutadiene; replotted from Menezes and Graessley [177]. $M_w = 350$ kg/mol; $M_w/M_n < 1.05$; concentration $= 0.0676$ g/cm^3 in Flexon 391, a hydrocarbon oil. *Source:* From "Nonlinear rheological behavior of polymer systems for several shear-flow histories," by E. V. Menezes and W. W. Graessley, *Journal of Polymer Science, Polymer Physics Edition*, Copyright © 1982 by John Wiley & Sons, Inc. Reprinted by permission of John Wiley & Sons, Inc.
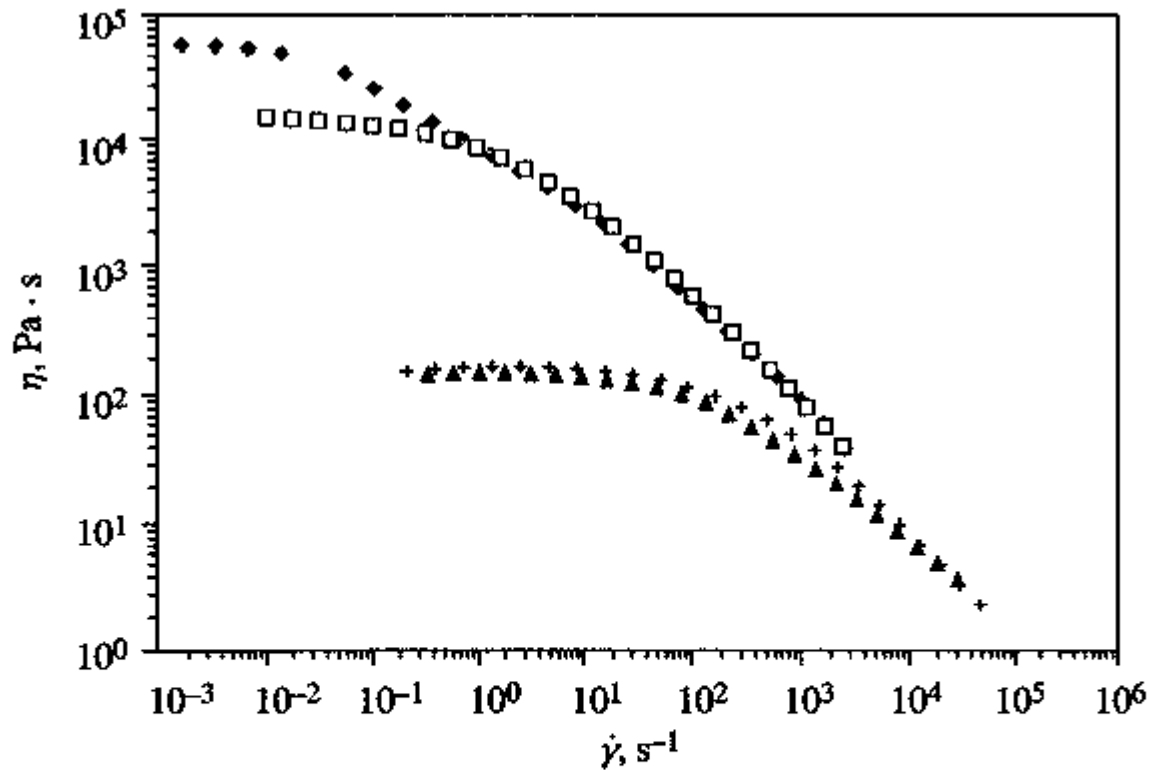
Figure 6.3 Shear viscosity η as a function of shear rate $\dot{\gamma}$ for linear and branched polydimethylsiloxanes. +, M_w=131 kg/mol, M_w/M_n=1.9, linear; $\triangle$, M_w=156 kg/mol, M_w/M_n=2.8, branched; $\square$, M_w=418 kg/mol, M_w/M_n=3.2, linear; $\diamondsuit$, M_w=428 kg/mol, M_w/M_n=2.9, branched; from Piau et al. [207]. *Source:* Reprinted from *Journal of Non-Newtonian Fluid Mechanics*, **30**, J. M. Piau, N. El Kissi, and B. Tremblay, "Low Reynolds number flow visualization of linear and branched silicones upstream of orifice dies," 197–232, Copyright © 1988, with permission from Elsevier Science.
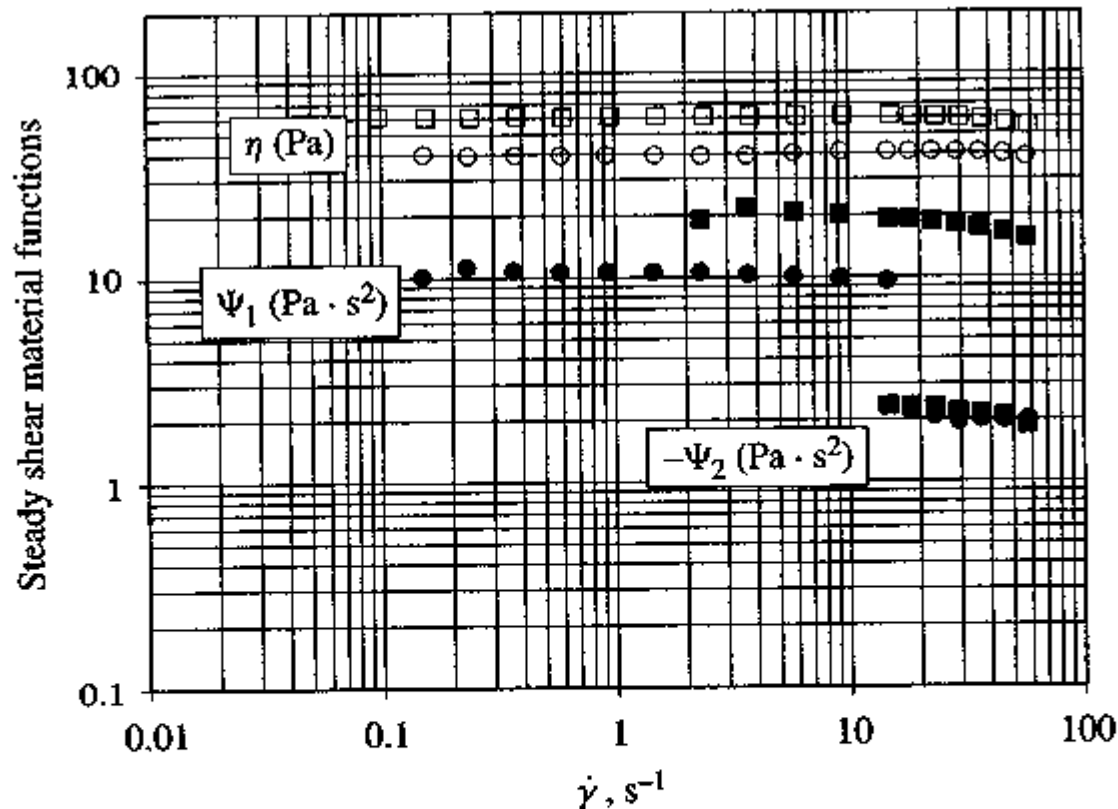
Figure 6.6 All three shear-flow material functions (η, Ψ_1, Ψ_2) as a function of shear rate for two polystyrene solutions; from Magda et al. [163]. $\bigcirc$, 28% polystyrene in dioctylpthalate (DOP); $\square$, 28% polystyrene in tricresylphosphate (TCP). The polystyrene in these solutions is broadly distributed with $M_w = 47$ kg/mol. *Source:* Reprinted with permission, "Rheology, flow instabilities, and shear-induced diffusion in polystyrene solutions," J. J. Magda, C. S. Lee, S. J. Muller, and R. G. Larson, *Macromolecules*, **26**, 1696–1706 (1993). Copyright © 1993, American Chemical Society.
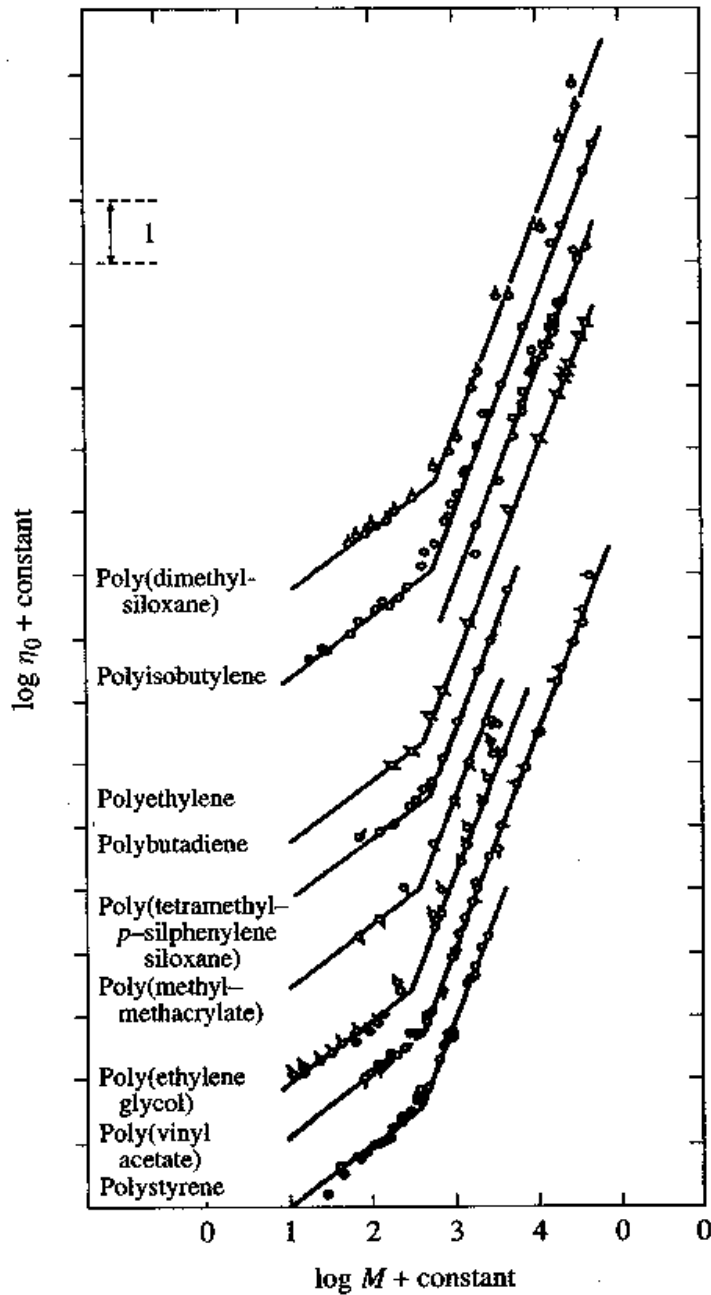
Figure 6.12 Effect of molecular weight on the measured zero-shear viscosity for a variety of polymers; from Berry and Fox [21]. Below a critical molecular weight M_c, $\eta_0 \propto M^1$; at higher molecular weights $\eta_0 \propto M^{3.4-3.5}$. *Source:* From "The viscosity of polymers and their concentrated solutions," G. C. Berry and T. G Fox, *Advances in Polymer Science*, 5, 261–357 (1968), Figure 1. Copyright © 1968, Springer-Verlag.
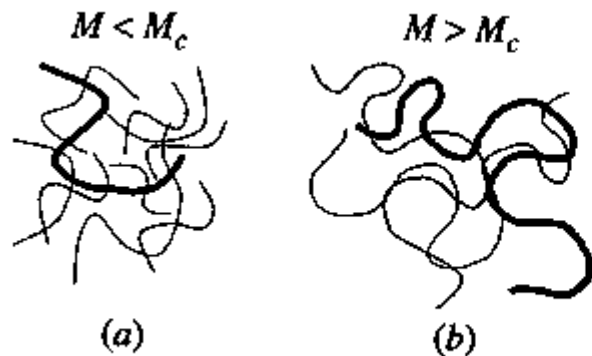
$M < M_c$ $M > M_c$

(a)   (b)

Figure 6.13 Schematic of (a) unentangled and (b) entangled polymers. Unentangled polymers are able to rapidly relax interactions with neighboring molecules. Entangled polymers form knots and are slowed down in their ability to relax interactions with their neighbors.
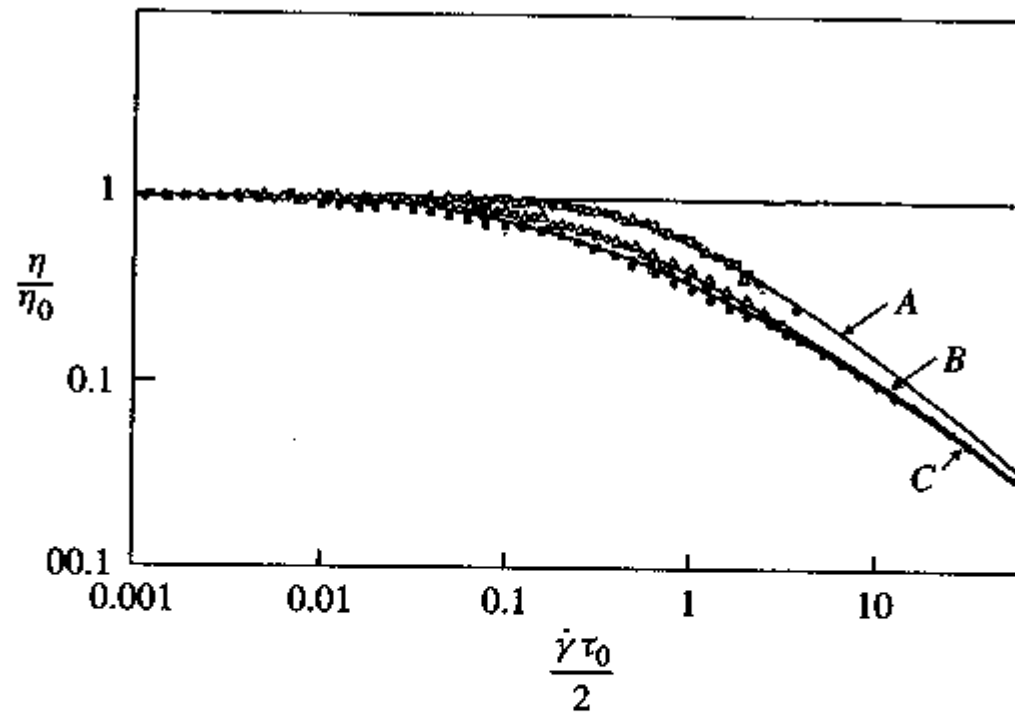
Figure 6.14 Effect of molecular weight distribution on viscosity; from Uy and Graessley [250a]. Shown are viscosity versus shear-rate master curves for poly(vinyl acetate) concentrated solutions in diethyl phthalate. Polymers of different M_w values were shifted empirically using the zero-shear viscosity η_0 and a time constant $\tau_0/2$ to produce the master curves for comparison. The different curves represent samples with different molecular weight distributions: A—$M_w/M_n = 1.09$; B—$M_w/M_n = 2.0$; C—branched. *Source:* Reprinted with permission, "Viscosity and normal stresses in poly(vinyl acetate) systems," W. C. Uy and W. W. Graessley, *Macromolecules*, 4, 458–463 (1971). Copyright © 1971, American Chemical Society.
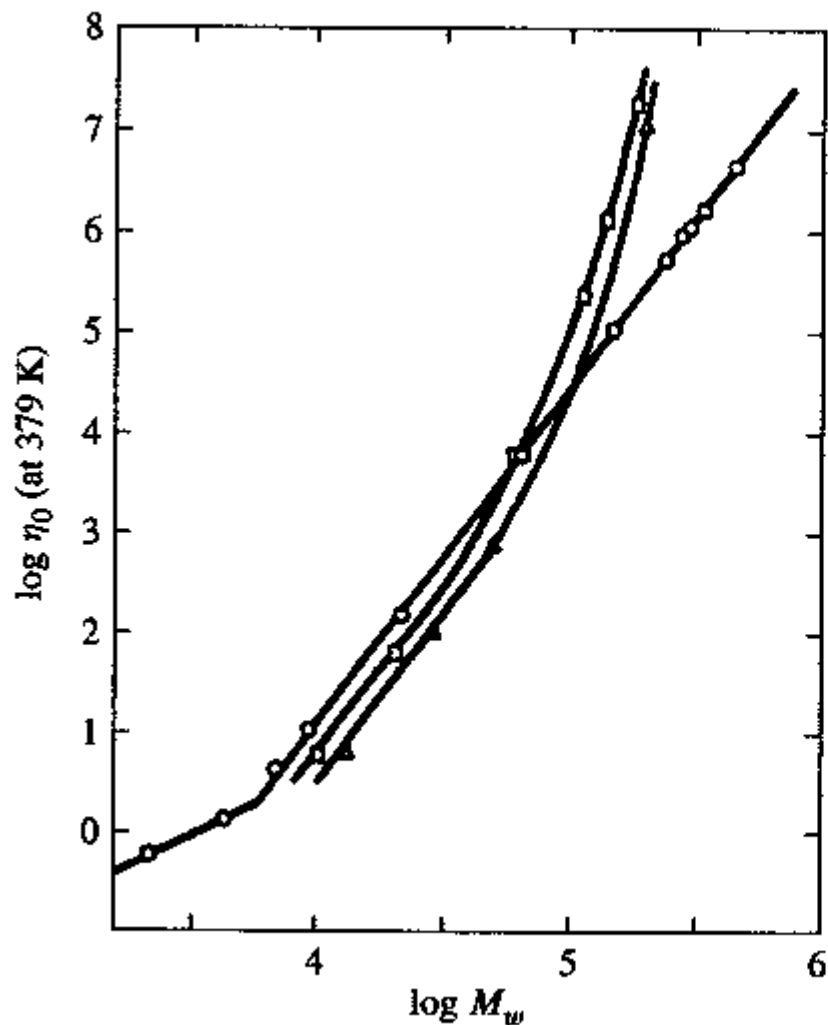
Figure 6.17 Effect of branching on zero-shear viscosity η_0, that is, at low shear rates; from Kraus and Gruver [131]. Curves are for ○ linear, □ three-armed star-branched (linear with one long side chain), and △ four-armed star-branched polybutadienes at 379 K. At lower molecular weights the branched polymers have lower η_0; at very high molecular weights, however, the viscosity of the branched polymers greatly exceeds that of the linear polymer. *Source:* From "Rheological properties of multichain polybutadienes," by G. Kraus and J. T. Gruver, *Journal of Polymer Science, Part A,* Copyright © 1965 by John Wiley & Sons, Inc. Reprinted by permission of John Wiley & Sons, Inc.
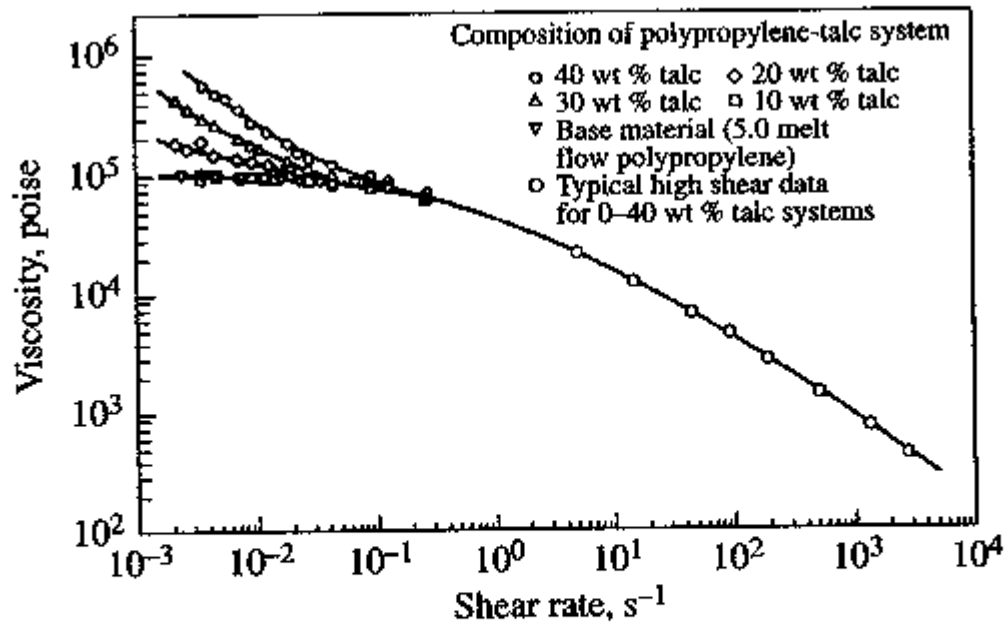
Figure 6.21 Viscosity versus shear rate at 200°C for talc-filled polypropylene; from Chapman and Lee [40]. Data at low rates were taken in a cone-and-plate rheometer; high-rate data were taken in a capillary rheometer. *Source:* From *SPE Journal,* Copyright © 1970, Society of Plastics Engineers. Reprinted by permission.
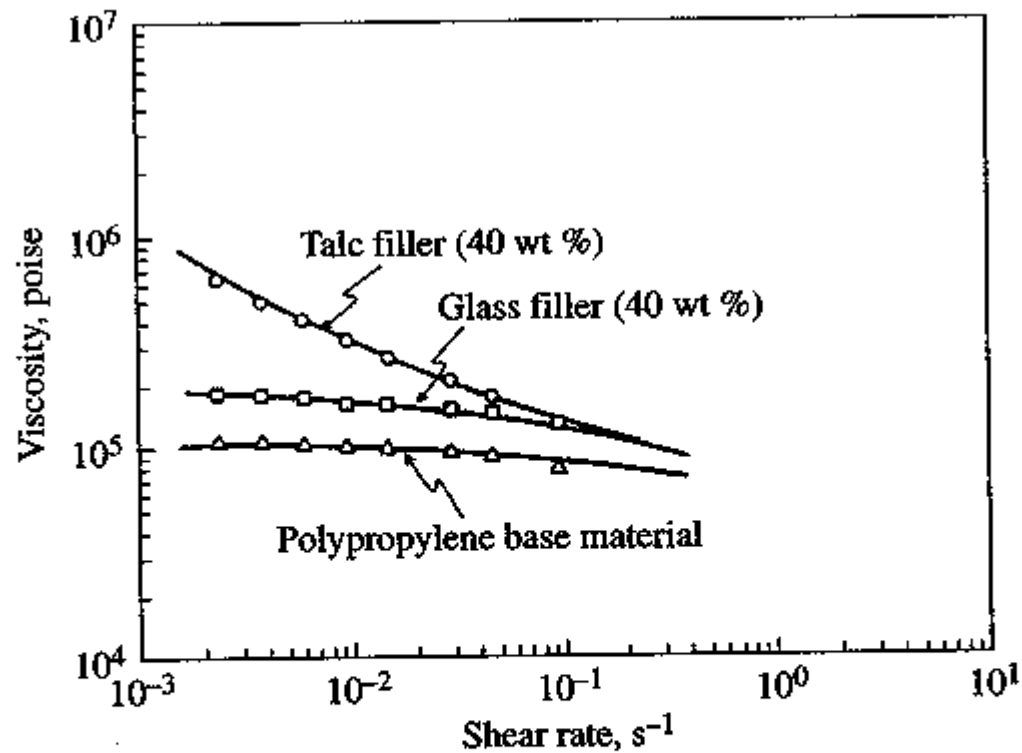
Figure 6.22 Viscosity versus shear rate for polypropylene and for polypropylene mixed with inert glass filler and interacting talc filler; from Chapman and Lee [40]. Although the absence of specific interactions reduces the viscosity of the glass-filled compared to the talc-filled polypropylene, the viscosity of the glass-filled system is still greater than that of the neat polymer. *Source:* From *SPE Journal*, Copyright © 1970, Society of Plastics Engineers. Reprinted by permission.
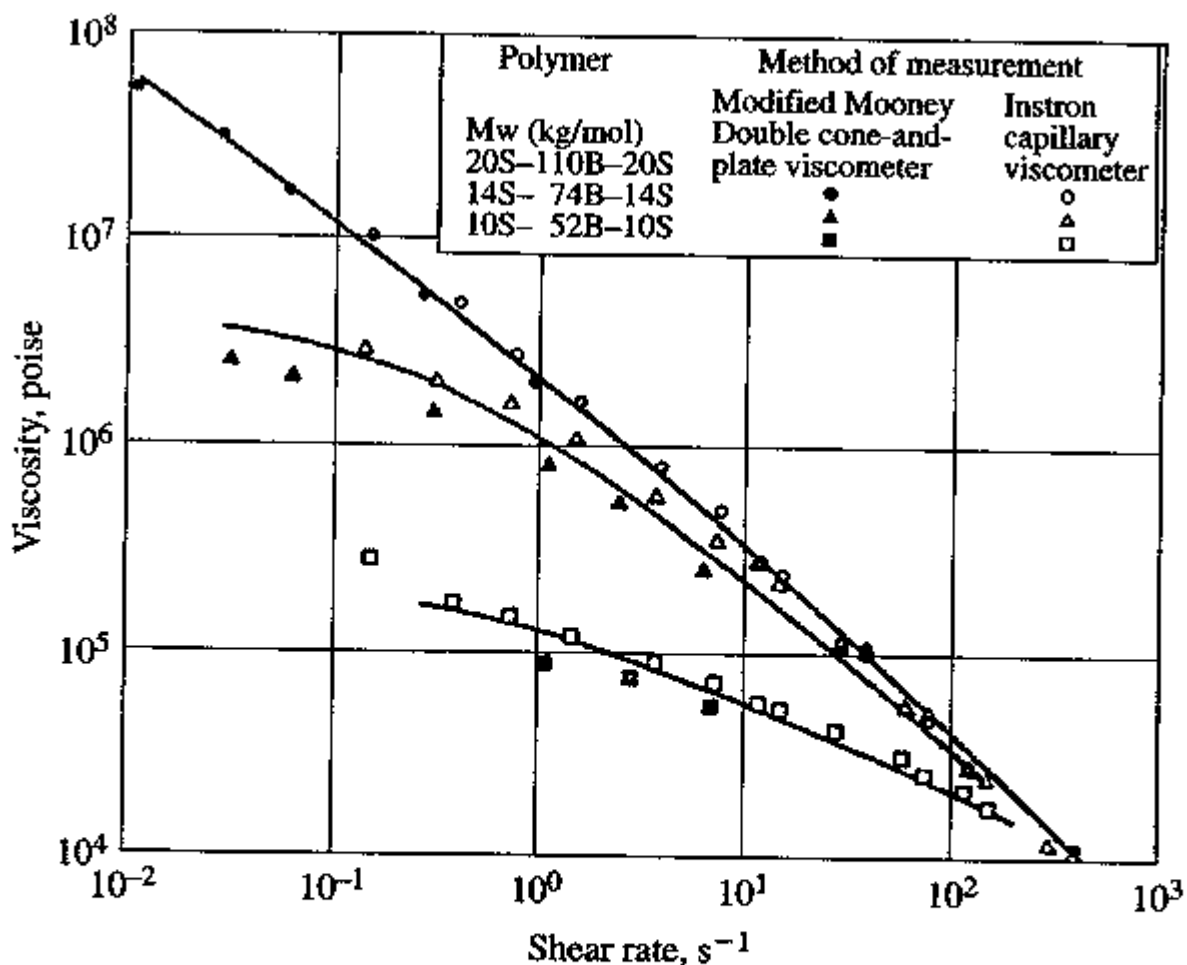
Figure 6.25 Steady shear viscosities versus shear rate of three (*b*)polystyrene–(*b*)polybutadiene–(*b*)polystyrene (SBS) triblock copolymers at 175°C; from Holden et al. [111]. Block molecular weights of each copolymer are also listed. *Source:* From "Thermoplastic elastomers," by G. Holden, E. T. Bishop and N. R. Legge, *Journal of Polymer Science, Part C,* Copyright © 1969 by John Wiley & Sons, Inc. Reprinted by permission of John Wiley & Sons, Inc.
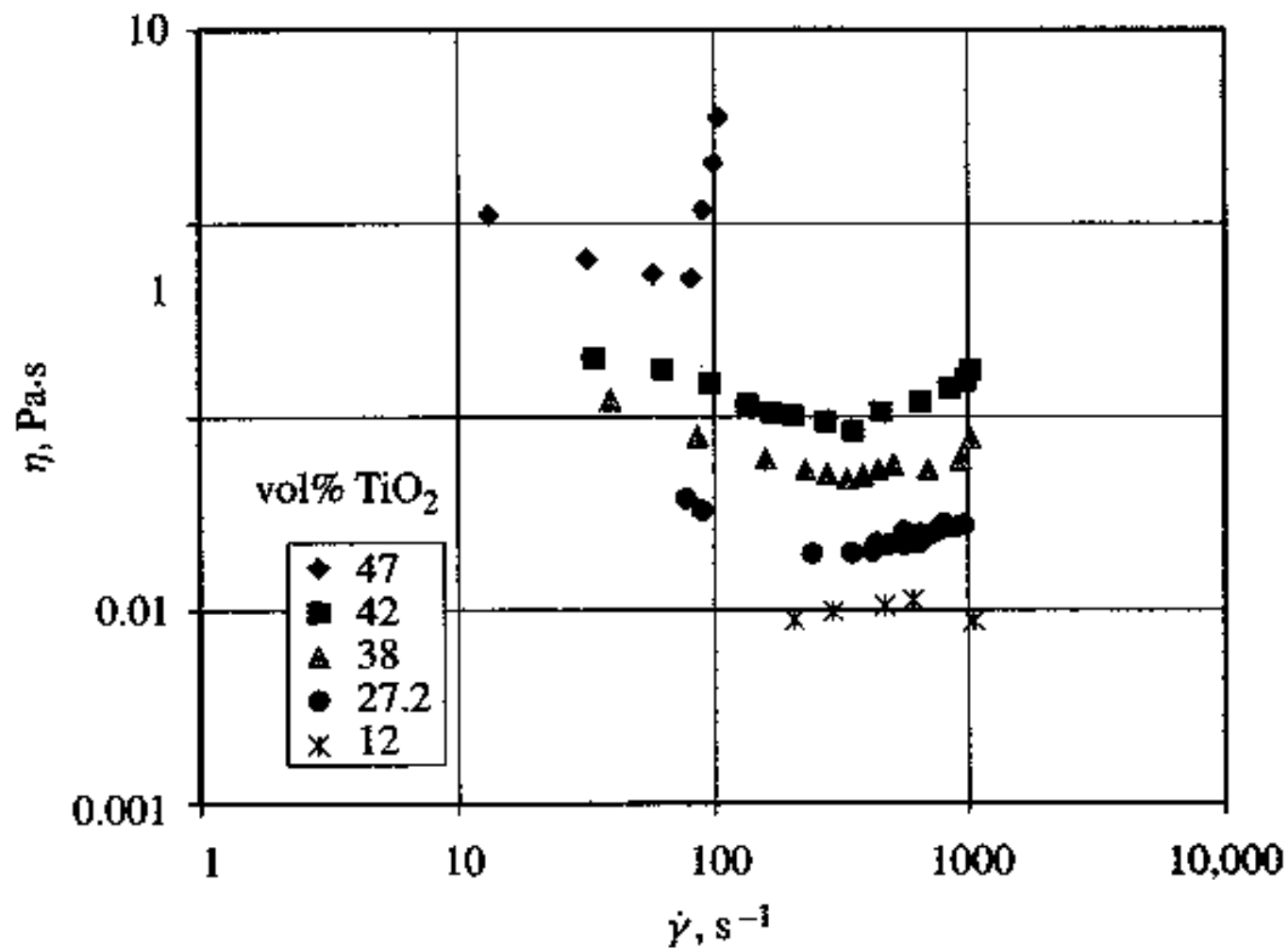
Figure 6.27 Viscosity versus shear rate for five suspensions of TiO$_2$ in water; recalculated and replotted from Metzner and Whitlock [178]. The diameters of the TiO$_2$ particles were between 0.2 and 1 μm, and the data were taken on a Couette (cup-and-bob) rheometer. *Source:* From the *Transactions of the Society of Rheology,* Copyright © 1958, The Society of Rheology. Reprinted by permission.
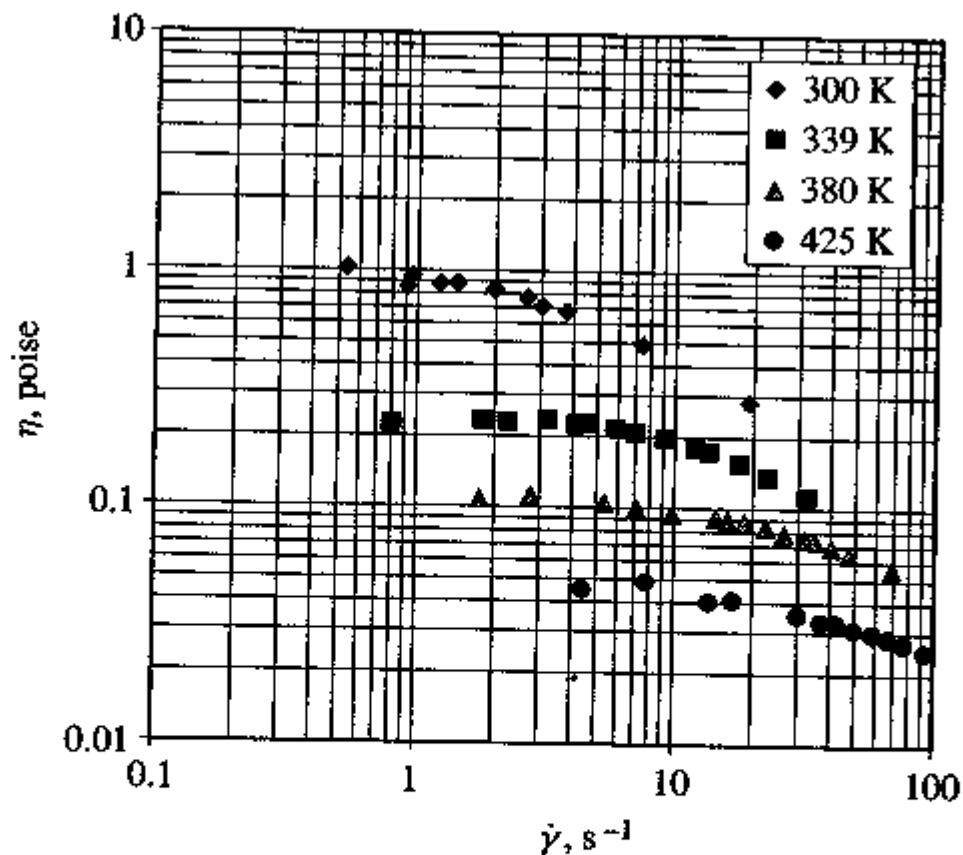
Figure 6.28 Viscosity versus shear rate at four different temperatures for a polybutadiene melt. Raw capillary data from Gruver and Kraus [102] corrected for nonparabolic velocity profile (Rabinowitsch correction; see Chapter 10) and plotted. $M_w = 145$ kg/mol, $M_w/M_n = 1.1$. From "Rheological properties of polybutadienes prepared by n-butyllithium initiation," by J. T. Gruver and G. Kraus, *Journal of Polymer Science, Part A*, Copyright © 1964 by John Wiley & Sons, Inc. Reprinted by permission of John Wiley & Sons, Inc.
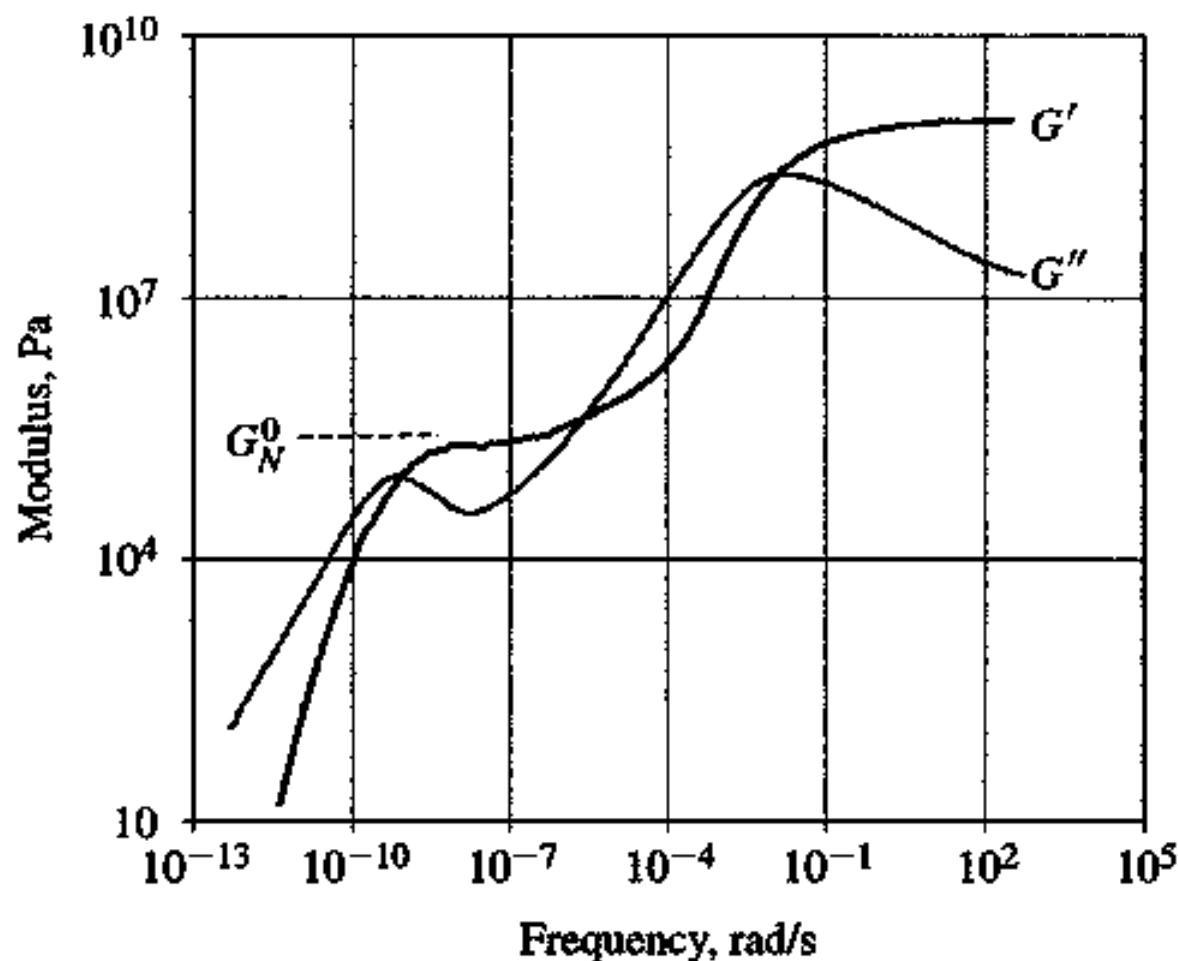
Figure 6.30 Master curve of the material functions $G'(\omega)$ and $G''(\omega)$ for an atactic linear polystyrene; data taken by D. J. Plazek and V. M. O'Rourke as plotted in Ferry [75]. $M_w = 600$ kg/mol, narrow molecular-weight distribution. The reference temperature is 100°C. *Source:* From *Viscoelastic Properties of Polymers*, J. D. Ferry, Copyright © 1980 by John Wiley & Sons. Reprinted by permission of John Wiley & Sons, Inc.
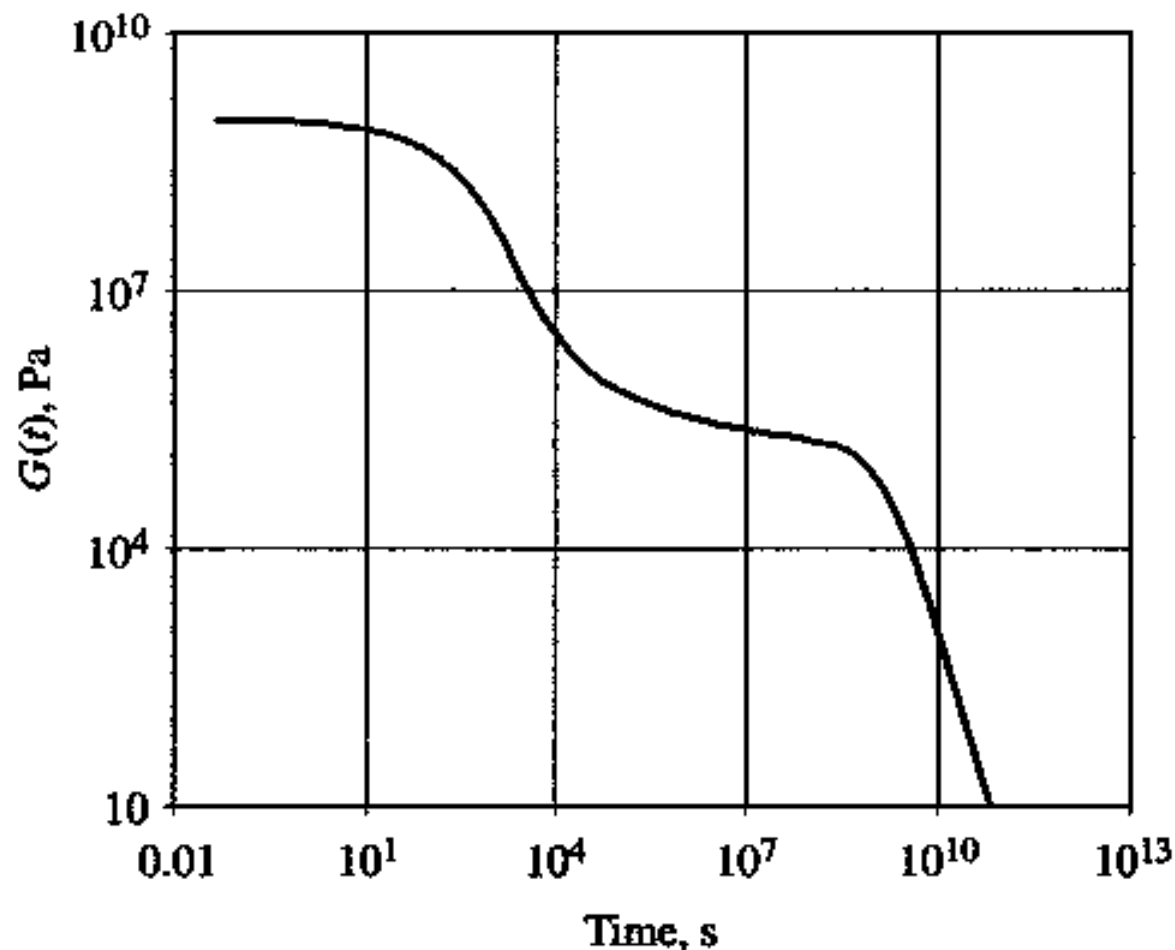
Figure 6.31 Master curve of the material function $G(t)$, the relaxation modulus, for an atactic linear polystyrene; calculated from the G' and G'' data in Figure 6.30 calculated by Ferry [75] from the data taken by D. J. Plazek and V. M. O'Rourke. The reference temperature is 100°C. *Source:* From *Viscoelastic Properties of Polymers*, J. D. Ferry, Copyright © 1980 by John Wiley & Sons. Reprinted by permission of John Wiley & Sons, Inc.
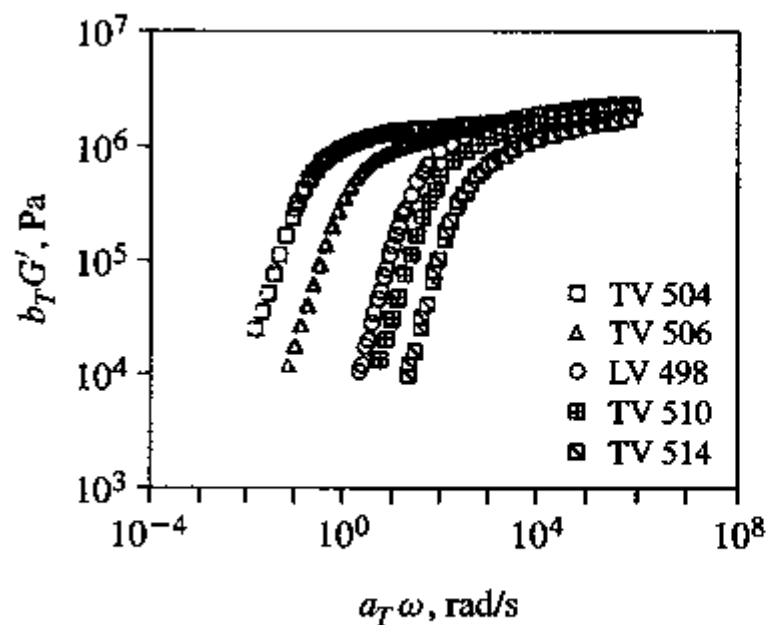
Figure 6.33 Master curves of storage modulus $b_T G'$ versus $a_T \omega$ for narrow-molecular-weight-distribution polybutadienes of various molecular weights; from Palade et al. [201]. b_T is the vertical shift factor, $b_T \equiv T_{ref}\rho_{ref}/T\rho$. Master curves were obtained from time–temperature superposition. $T_{ref} = 25°C$, M_w (kg/mol): TV504 = 464, TV506 = 229, LV498 = 85.8, TV510 = 70.6, TV514 = 51.3. *Source:* Reprinted with permission, "Time–temperature superposition and linear viscoelasticity of polybutadienes," L. I. Palade, V. Verney, and P. Attane, *Macromolecules*, **28**, 7051–7057 (1995). Copyright © 1995, American Chemical Society.
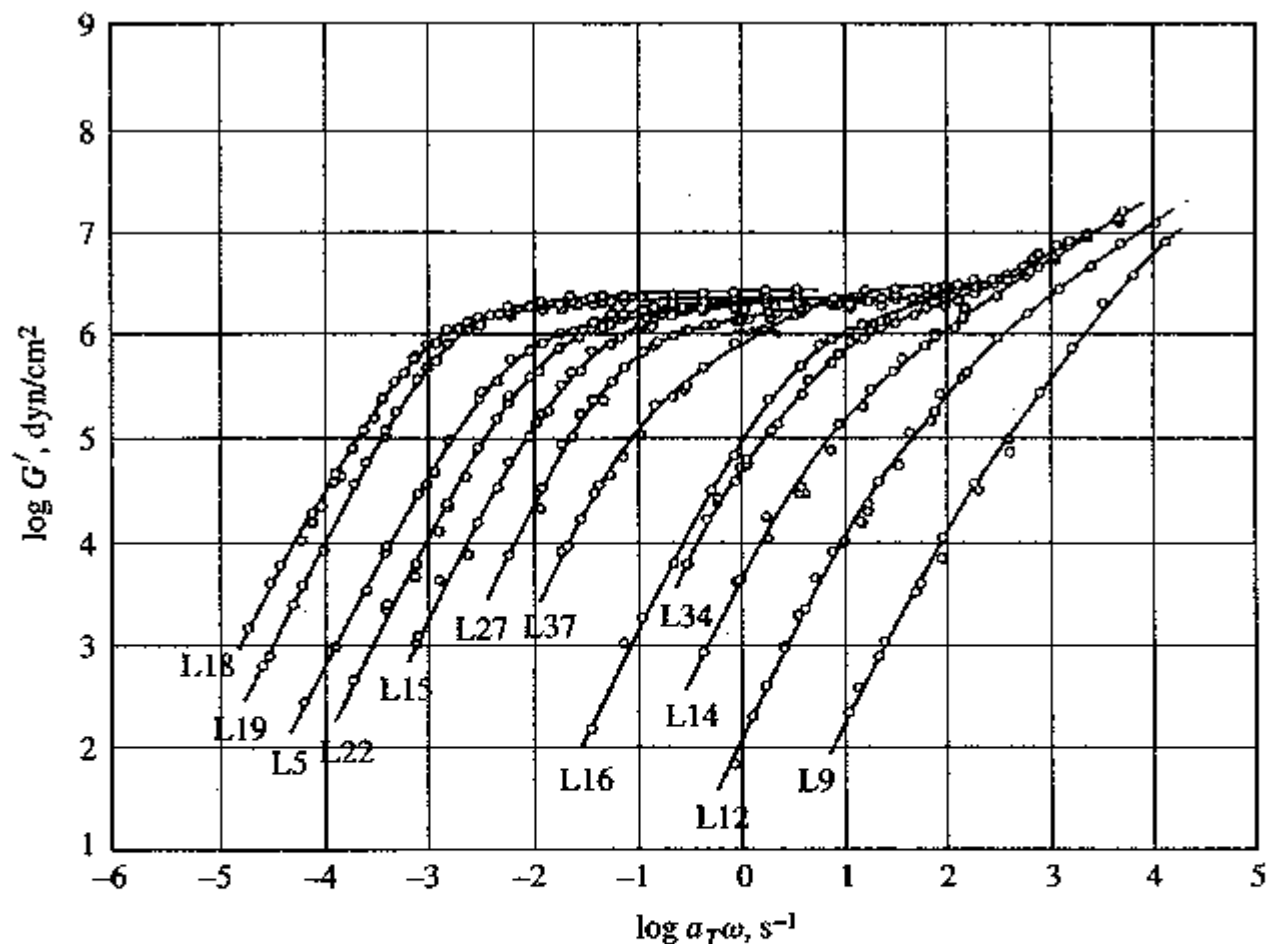
Figure 6.34 Master curves of storage modulus G' versus $a_T\omega$ for narrow-molecular-weight-distribution polystyrenes of various molecular weights; from Onogi et al. [196]. Master curves were obtained from time–temperature superposition. $T_{\text{ref}} = 160°\text{C}$, M_w (kg/mol): L18 = 581, L19 = 513, L5 = 351, L22 = 275, L15 = 215, L27 = 167, L37 = 113, L16 = 58.7, L34 = 46.9, L14 = 28.9, L12 = 14.8, L9 = 8.9. *Source:* Reprinted with permission, "Rheological properties of anionic polystyrenes. I. Dynamic viscoelasticity of narrow-distribution polystyrenes," Onogi, S., T. Masuda, and K. Kitagawa, *Macromolecules*, **3**, 109–116 (1970). Copyright © 1970, American Chemical Society.
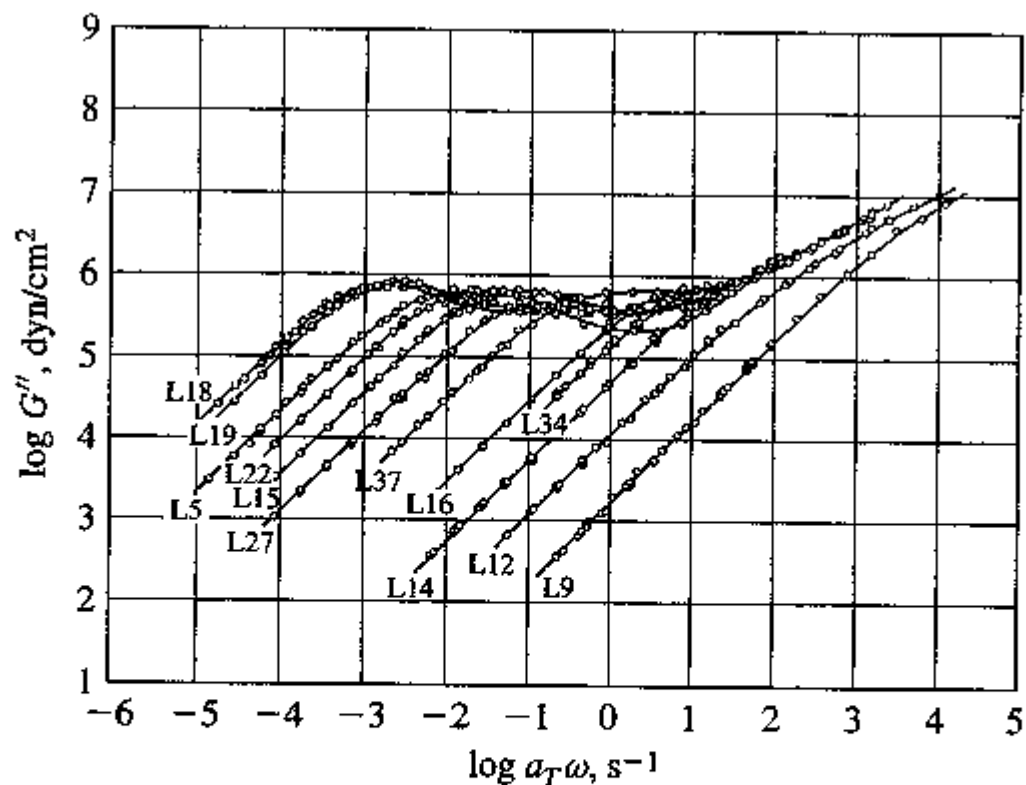
Figure 6.36 Master curves of loss modulus G'' versus $a_T\omega$ for narrow-molecular-weight-distribution polystyrenes of various molecular weights; from Onogi et al. [196]. Master curves were obtained from time–temperature superposition. $T_{ref} = 160°C$; M_w listed in Figure 6.34. *Source:* Reprinted with permission, "Rheological properties of anionic polystyrenes. I. Dynamic viscoelasticity of narrow-distribution polystyrenes," Onogi, S., T. Masuda, and K. Kitagawa, *Macromolecules*, **3**, 109–116 (1970). Copyright © 1970, American Chemical Society.
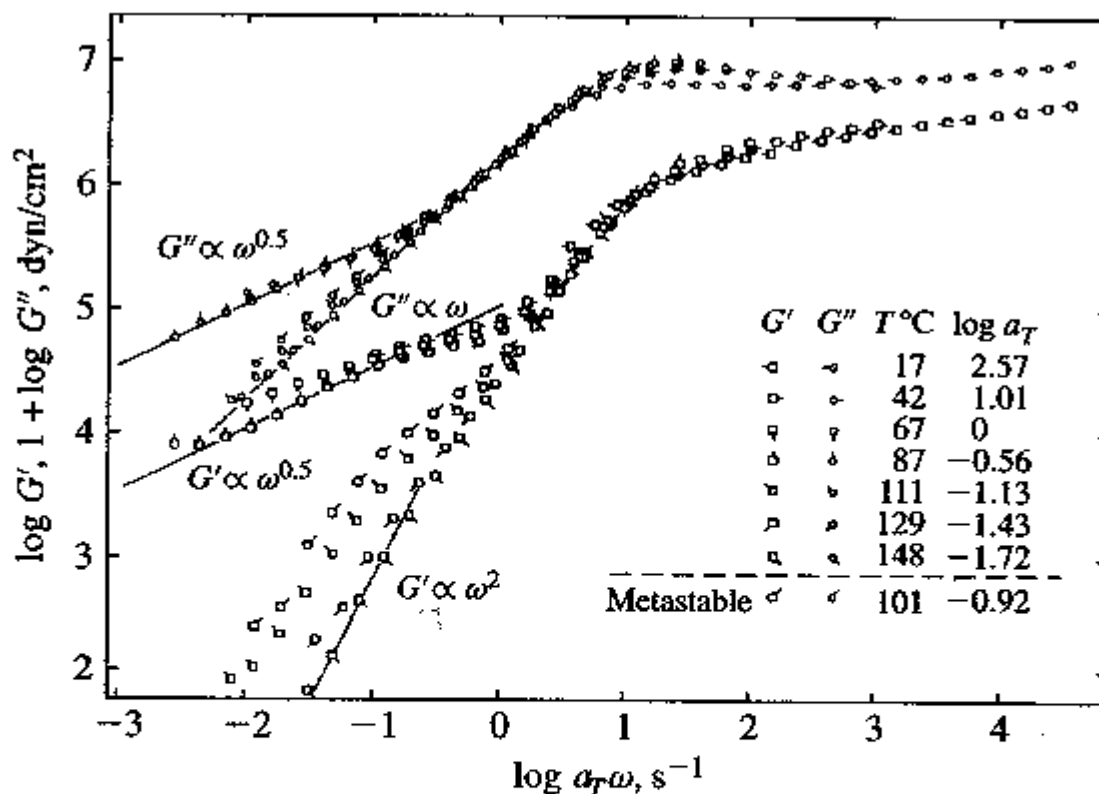
Figure 6.41 Linear viscoelastic moduli $G'(\omega)$ and $G''(\omega)$ for a 1,4-polybutadiene–1,2-polybutadiene block copolymer (block M_w =27.3–44.5 kg/mol) [14]; from Bates. The data have been time–temperature shifted to a reference temperature of 67°C. Near 100°C the microphase structure is melted, and at the highest temperature shown $G' \propto \omega^2$ and $G'' \propto \omega^1$. *Source:* Reprinted with permission, "Block copolymers near the microphase separation transition. 2. Linear dynamic mechanical properties," F. Bates, *Macromolecules*, **17**, 2607–2613 (1984). Copyright © 1984, American Chemical Society.
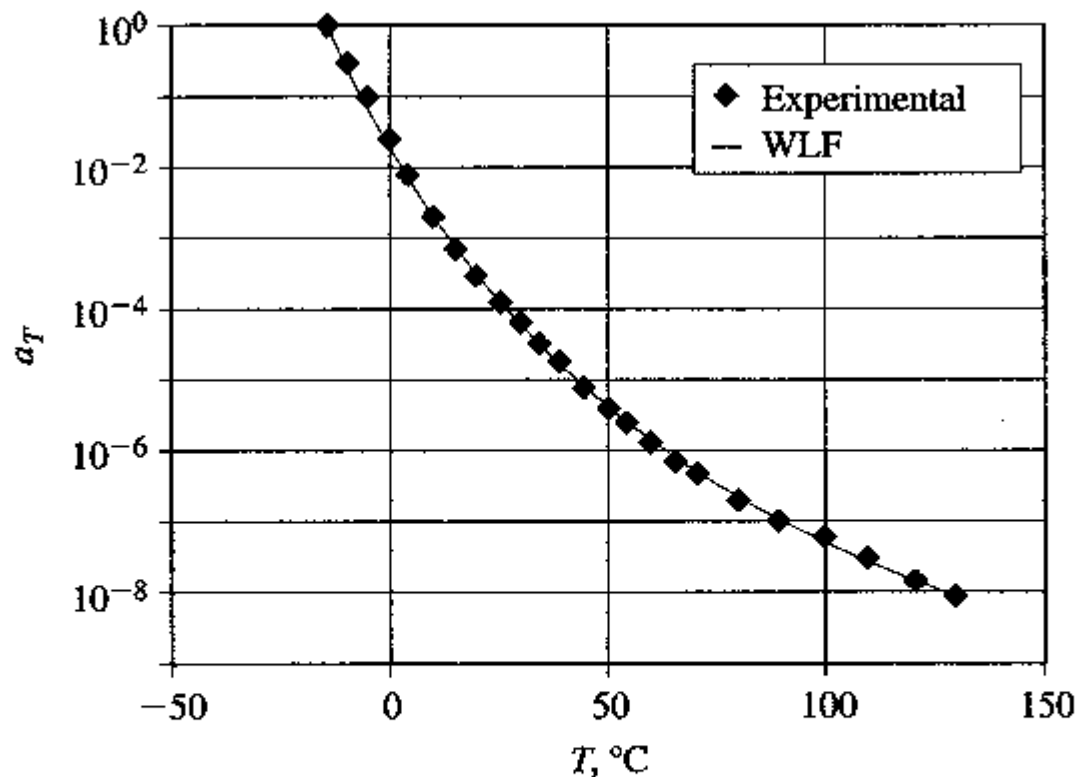
Figure 6.45 Shift parameters versus temperature for poly (*n*-octyl methacrylate) in Figure 6.44; $T_{ref} = -14.3°C = 258.9K$. Also included is the fit to the WLF equation; calculated from data in Dannhauser et al. [56]. *Source:* From the *Journal of Colloid Science*, Copyright © 1958, Academic Press. Reprinted by permission.
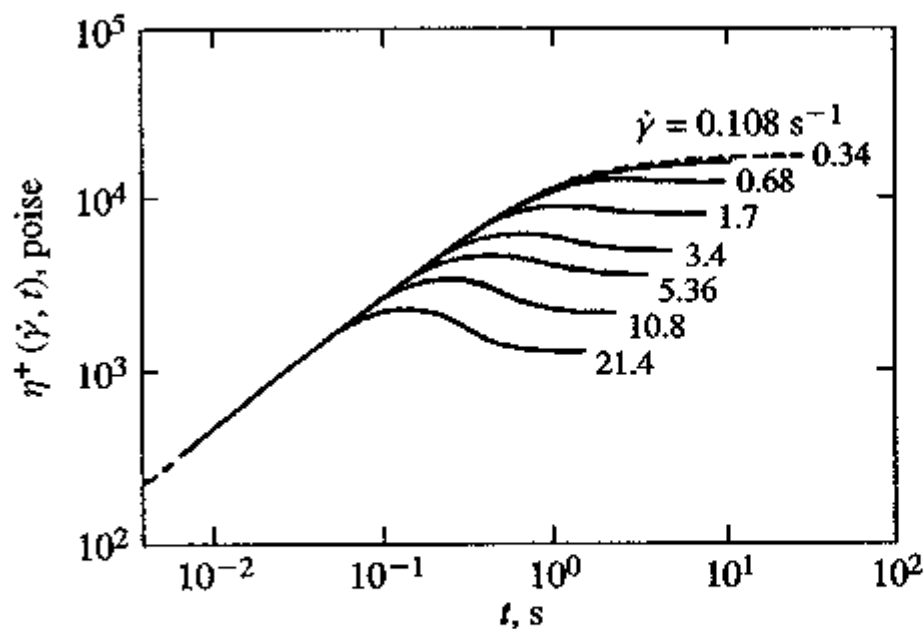
Figure 6.49 Shear-stress growth function as a function of time t at several shear rates for a concentrated solution of a narrowly distributed polybutadiene; from Menezes and Graessley [177]. $M_w = 350$ kg/mol; $M_w/M_n < 1.05$; concentration = 0.0676 g/cm^3 in Flexon 391, a hydrocarbon oil. *Source:* From "Nonlinear rheological behavior of polymer systems for several shear-flow histories," by E. V. Menezes and W. W. Graessley, *Journal of Polymer Science, Polymer Physics Edition,* Copyright © 1982 by John Wiley & Sons, Inc. Reprinted by permission of John Wiley & Sons, Inc.
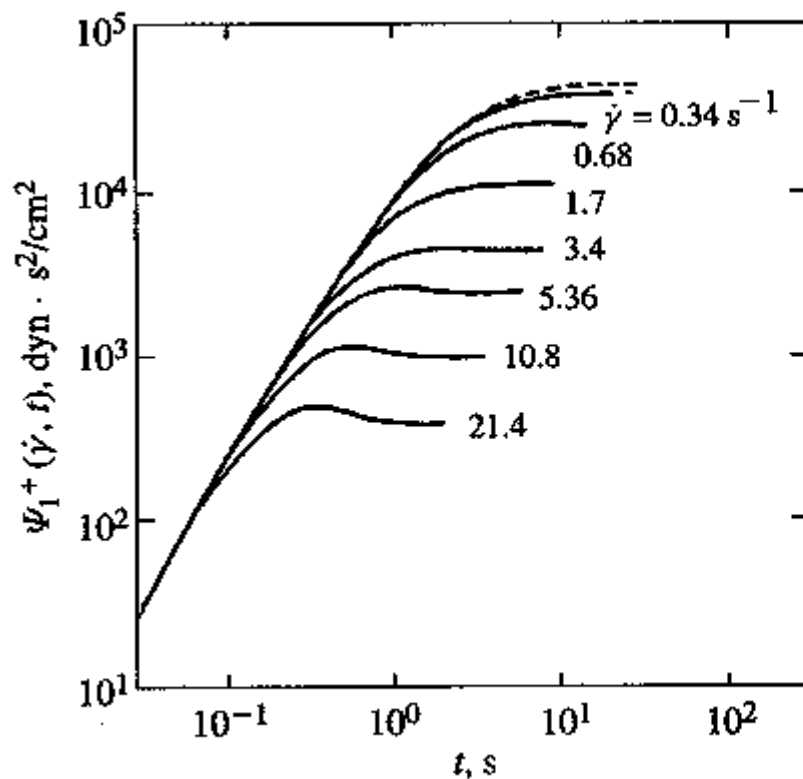
Figure 6.50 First normal-stress growth function as a function of time t at several shear rates for a concentrated solution of a narrowly distributed polybutadiene; from Menezes and Graessley [177]. $M_w = 350$ kg/mol, $M_w/M_n < 1.05$; concentration $= 0.0676$ g/cm^3 in Flexon 391, a hydrocarbon oil. *Source:* From "Nonlinear rheological behavior of polymer systems for several shear-flow histories," by E. V. Menezes and W. W. Graessley, *Journal of Polymer Science, Polymer Physics Edition*, Copyright © 1982 by John Wiley & Sons, Inc. Reprinted by permission of John Wiley & Sons, Inc.
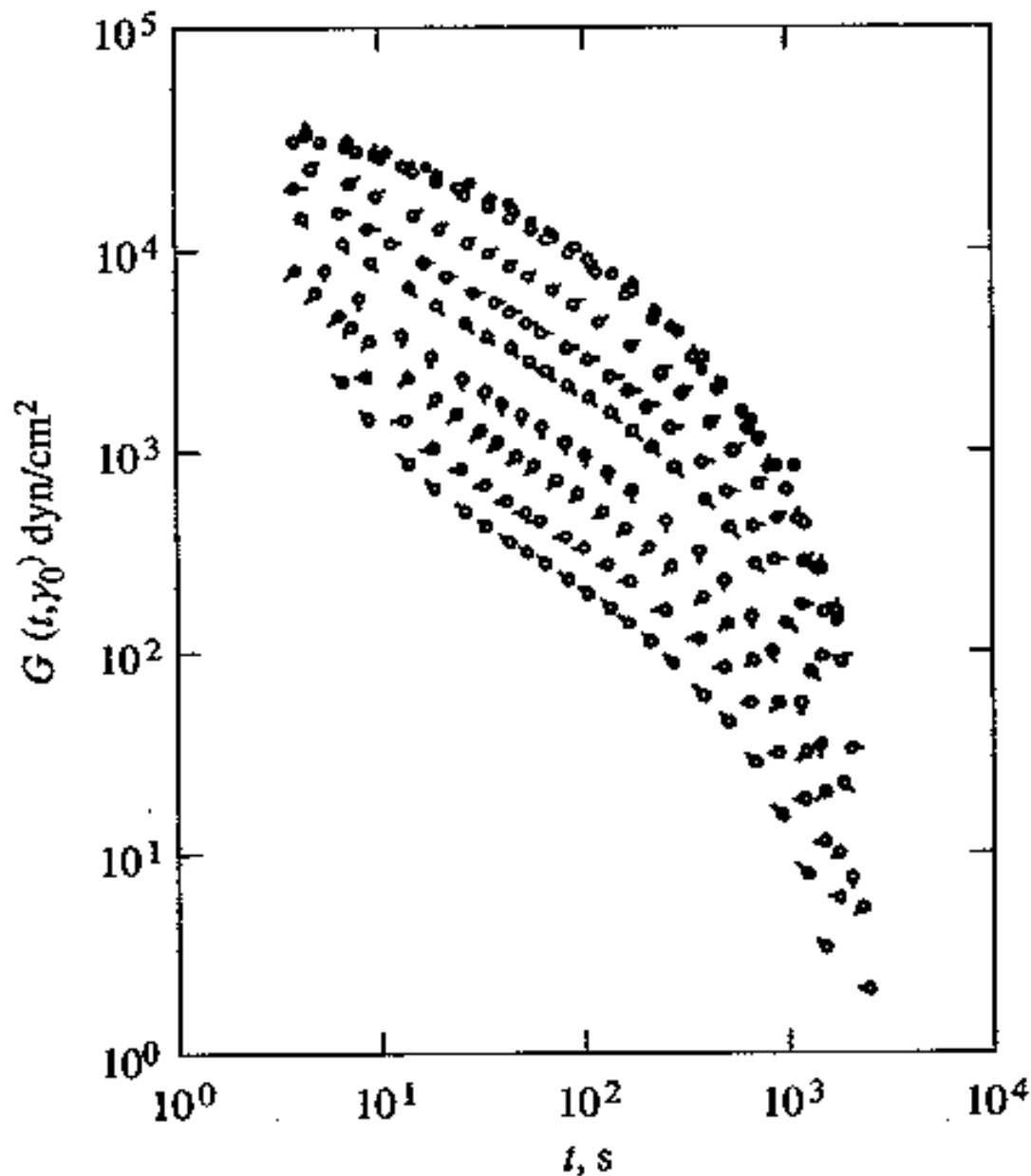
Figure 6.57 Nonlinear shear relaxation modulus $G(t, \gamma_0)$ as a function of time t at 33.5°C, measured in relaxation after step shear strain for 20% solutions of narrow molecular-weight-distribution polystyrene ($M_w = 1.8 \times 10^6$) in chlorinated diphenyl; from Einaga et al. [72]. Different curves are for different strain amplitudes γ_0: ○, $\gamma_0 = 0.41$; pip up $\gamma_0 = 1.87$; for successive clockwise 45° rotations of pip, $\gamma_0 = 3.34, 5.22, 6.68, 10.0, 13.4, 18.7$, and 25.4. *Source:* From *Polymer Journal*, Copyright © 1971, The Society of Polymer Science, Japan. Reprinted by permission.
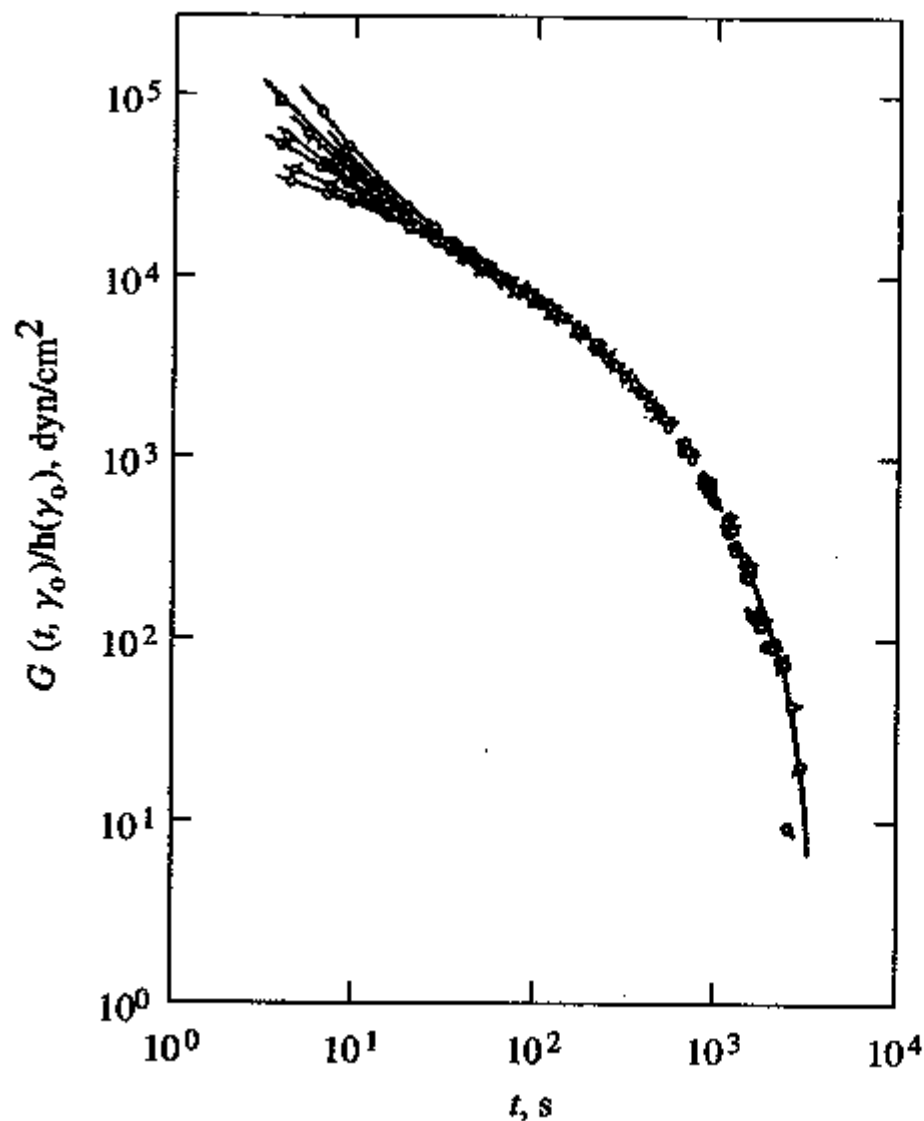
Figure 6.58 Shifted relaxation modulus $G(t, \gamma_0)/h(\gamma_0)$ at 33.5°C for the polystyrene solution data shown in Figure 6.57; from Einaga et al. [72]. $h(\gamma_0)$ is the damping function and is equal to $G(t, \gamma_0)/G(t)$, where $G(t)$ is the relaxation modulus at small strains, and $\log h$ is the vertical shift required to superpose the curves of Figure 6.57. Symbols are the same as in Figure 6.57. *Source:* From *Polymer Journal*, Copyright © 1971, The Society of Polymer Science, Japan. Reprinted by permission.
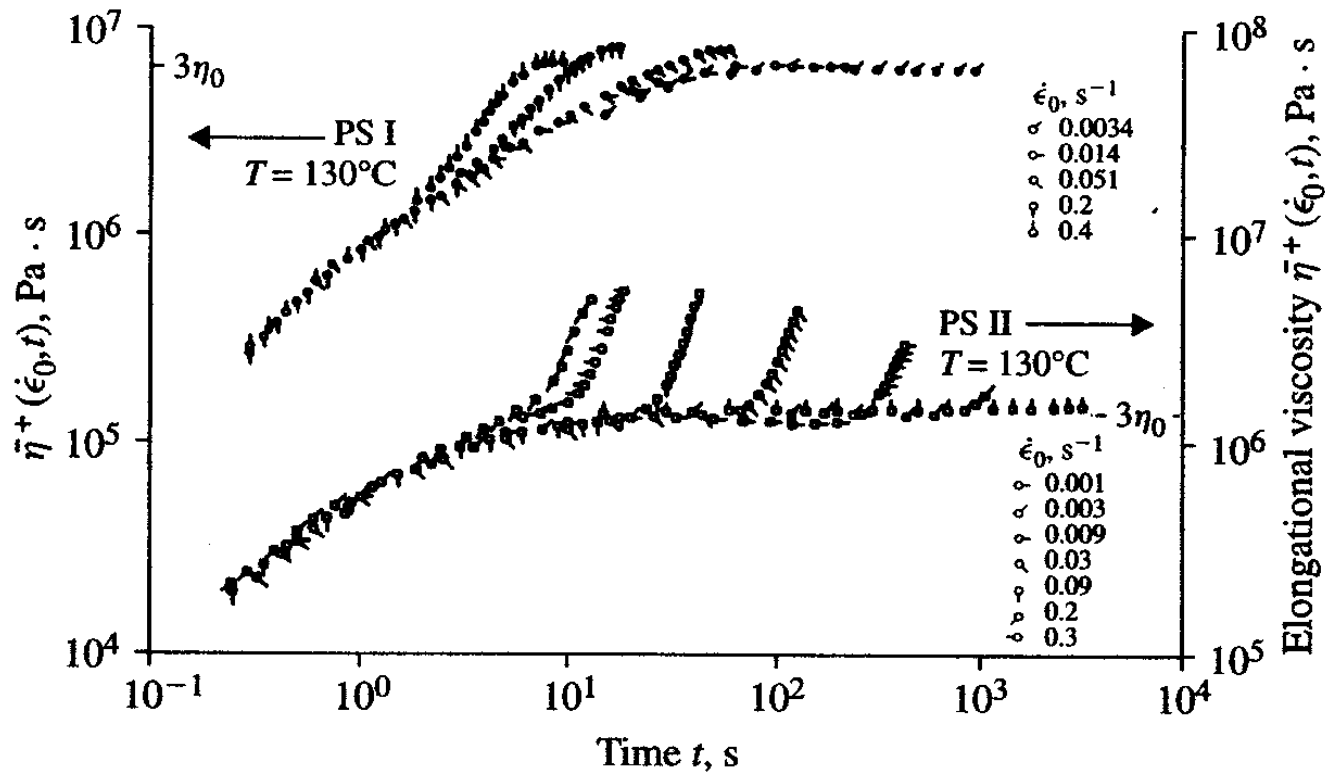
Figure 6.62 Start-up uniaxial elongational viscosity $\bar{\eta}^+(t, \dot{\epsilon}_0)$ versus time t for two polystyrenes at 130°C; from Münstedt [187]. For PS I, $M_w = 74$ kg/mol, $M_w/M_n = 1.2$; for PS II, $M_w = 39$ kg/mol, $M_w/M_n = 1.1$. *Source:* From the *Journal of Rheology*, Copyright © 1980, The Society of Rheology. Reprinted by permission.
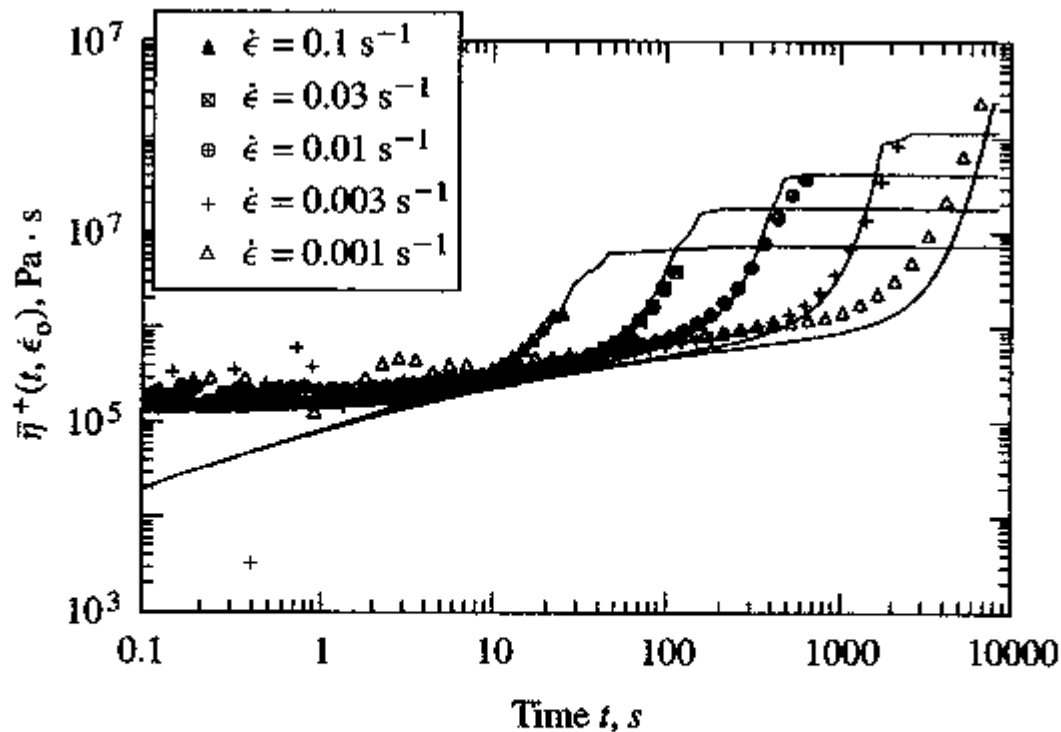
Figure 6.63 Start-up uniaxial elongational viscosity, $\bar{\eta}^+(t, \dot{\epsilon}_0)$ versus time t for low-density polyethylene at 140°C, $M_w = 250$ kg/mol, $M_w/M_n = 15$; from Inkson et al. [130a]. Solid curves represent a fit to a molecular constitutive equation called the 12 mode pompom melt. *Source:* From the *Journal of Rheology*, Copyright © 1999, The Society of Rheology. Reprinted by permission.
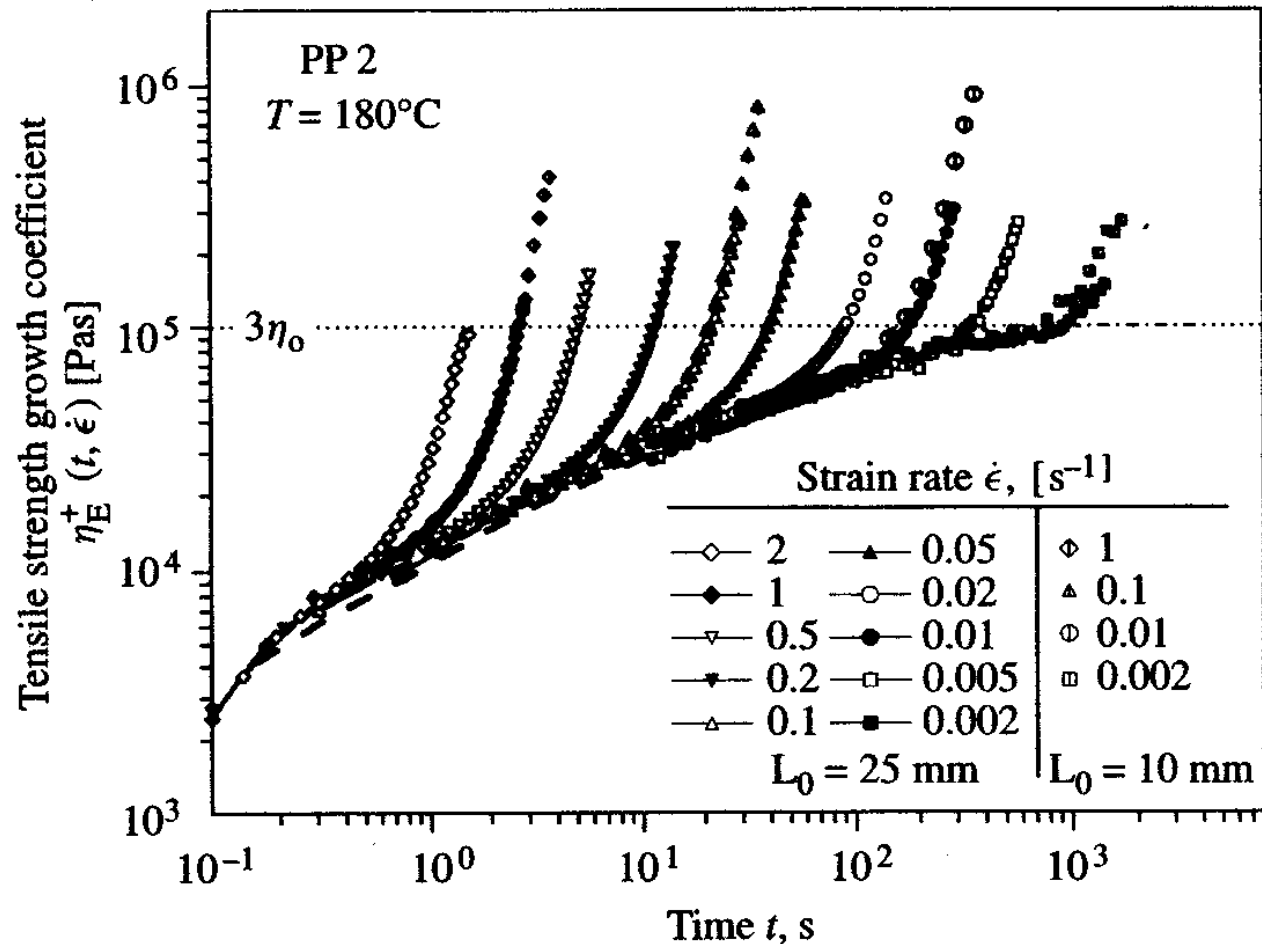
Figure 6.64 Start-up uniaxial elongational viscosity, $\bar{\eta}^+(t, \dot{\epsilon}_0)$, versus time t for polypropylene at 180°C; from Kurzbeck et al. [135]. Two initial sample lengths were used, $L_0 = 25$ mm and 10 mm as indicated on the figure. *Source:* From the *Journal of Rheology,* Copyright © 1999, The Society of Rheology. Reprinted by permission.